

DESIGN METHODOLOGY OF MULTI-FREQUENCY UNEQUAL SPLIT WILKINSON POWER DIVIDERS USING TRANSMISSION LINE TRANSFORMERS

A. Qaroot and N. Dib

Electrical Engineering Department
Jordan University of Science and Technology
P. O. Box 3030, Irbid 22110, Jordan

A. Gheethan

Electrical Engineering Department
South Dakota School of Mines and Technology
Rapid City, SD, USA

Abstract—In this paper, a new simple design procedure of multi-frequency unequal split Wilkinson power dividers (WPDs) is presented. The procedure is based on using N -sections of transmission line transformers, instead of the conventional quarter-wave WPD branches, to realize a WPD that operates at N frequencies. Good isolation is achieved by using lumped resistors without any extra modification to the conventional structure of WPDs. The analysis, design procedure, and mathematical expressions are presented for arbitrary design frequencies, and arbitrary power split ratio. For verification purposes, a 1 : 2 dual-frequency, a 1 : 2 tri-frequency, and a 1 : 2 quad-frequency WPDs are designed and fabricated. The measured results show good agreement with those obtained using the presented design methodology and with full-wave simulated results.

1. INTRODUCTION

With the emergence of multi-band applications, such as wireless communications, the need for multi-frequency microwave components has become highly demanded. One such widely used component is the Wilkinson power divider (WPD) [1, 2]. Recently, the dual-frequency operation of unequal split WPD has been a hot research topic. Several

Corresponding author: N. Dib (nihad@just.edu.jo).

different structures have been proposed in the literature. Feng [3] proposed a simple structure for a dual-frequency unequal split WPD. However, the conditions required to match the output ports (S_{22} and S_{33}) were not presented. These conditions play an important role in the design of efficient WPDs. Moreover, a single resistor was only used, which did not provide good isolation between the output ports. Other structures were proposed [4–6], which employed extra transmission line sections and/or reactive components that make the design and its realization even more complicated. In [7], Oraizi presented the design of broadband asymmetric multi-section WPDs. After a rather extensive mathematical derivation, an optimization process was used to find the values of the design parameters. In [8–10], equal split multi-frequency WPDs were studied. To our knowledge, the design of tri-frequency and quad-frequency *unequal split* WPDs has not been presented before in the literature.

In this paper, a general procedure for the design of multi-frequency unequal split 2-way WPDs is described. Dual-frequency, triple-frequency, and quad-frequency unequal split WPDs are designed and fabricated to verify the proposed design method. These designs are achieved by replacing the quarter-wave branches of a conventional unequal power divider by transmission line transformers consisting of two sections (in the case of dual-frequency divider), three sections (in the case of triple-frequency divider), and four sections (in the case of quad-frequency divider). The particle swarm optimization (PSO) [11] technique is utilized to obtain the appropriate characteristic impedances and lengths of these sections. In our analysis, simple matching equations have to be satisfied numerically at the desired frequencies. For the dual-frequency case, the design is even simpler using Monzon's theory [12]. For completeness, all the expressions needed to accomplish the design are presented in this paper. To verify the design procedure, a 1 : 2 dual-frequency, a 1 : 2 tri-frequency, and a 1 : 2 quad-frequency WPDs are designed and fabricated. The measured results show good agreement with those obtained using the presented design methodology and with full-wave simulated results.

2. GENERAL DESIGN PROCEDURE

Figure 1 shows the general topology of the proposed multi-frequency unequal split WPD. This configuration realizes unequal power split ratio at N arbitrary frequencies. N sections of transmission line transformers (TLTs) are used at the two branches to achieve proper matching at the desired frequencies. Moreover, N resistors are used to obtain good isolation between the output ports at the design

frequencies. Based on Parad’s theory [13], the even-odd mode analysis can be adapted to carry out the analysis. When two signals are applied at the output ports 2 and 3, with same amplitude and phase (even mode), the circuit can be modeled as two separate transmission line transformers [14], and the isolation resistors are open circuited as shown in Figure 2. This mode can be used to find the characteristic impedances and electrical lengths of the TLTs by imposing the matching condition at the input or output ports. On the other hand, applying equal amplitude, 180° out of phase signals at the output ports 2 and 3 gives the odd mode. In this mode, the circuit can be modeled as a series connection of transmission lines and parallel resistors as illustrated in Figure 3. The isolation resistors are grounded in this mode. By applying the matching condition at the output ports, the values of the isolation resistors can be found. It is worth mentioning that in our analysis, it is assumed that the cross-sectional dimensions of the microstrip/strip lines are relatively small with respect to wavelength, so that the effect of the discontinuities caused by corners and junctions on the performance of the designs is neglected [13]. The details of this even-odd mode analysis are presented in the following sub-sections.

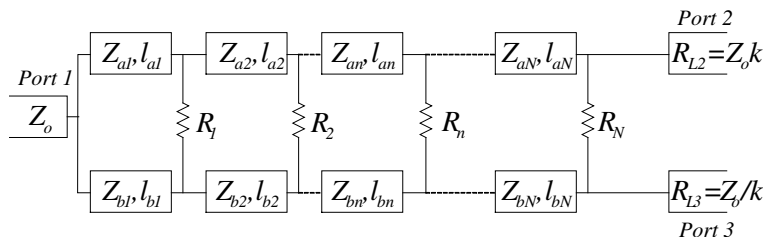


Figure 1. General structure of a multi-frequency unequal split WPD.

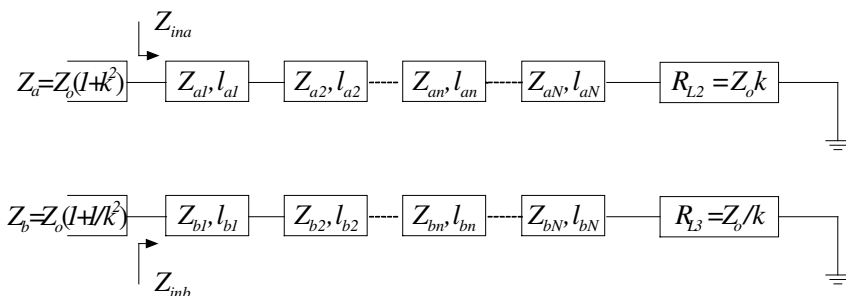


Figure 2. Even mode equivalent circuit for the proposed multi-frequency unequal split WPD.

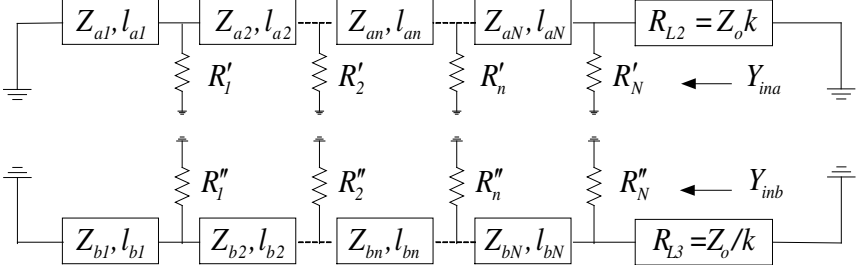


Figure 3. Odd mode equivalent circuit for the proposed multi-frequency unequal split WPD.

2.1. Even Mode Analysis

In the even mode (Figure 2), the characteristics impedances (Z 's) and physical lengths (l 's) of the transmission line sections can be found by applying the matching condition at the input port, where the input impedance at the input port should satisfy the following two conditions:

$$Z_{ina} = Z_a = Z_0(1 + k^2) \quad (1)$$

$$Z_{inb} = Z_b = Z_0 \left(1 + \frac{1}{k^2} \right) \quad (2)$$

where k^2 is the power split ratio between the two output ports (P_3/P_2). The input impedances Z_{ina} and Z_{inb} can be easily found using transmission line theory. Our objective is to find the lengths and impedances of the N transmission line sections such that a perfect match is obtained at the N desired frequencies. Equations (1) and (2) are non-linear, and thus, in general, an optimization process is needed to solve them. For dual-frequency operation, a closed form solution can be obtained using Monzon's theory [12], while an analysis similar to that in [15, 16] can be used to analyze the tri-frequency and quad-frequency designs.

2.2. Odd Mode Analysis

When applying the odd mode excitation, the circuit shown in Figure 1 is bisected by grounding the plane of symmetry as shown in Figure 3. By imposing the matching condition at the output ports 2 and 3, the input admittances seen looking into ports 2 and 3 should satisfy the

following conditions:

$$Y_{ina} = \frac{1}{R_{L2}} \tag{3}$$

$$Y_{inb} = \frac{1}{R_{L3}} \tag{4}$$

These two conditions must be satisfied simultaneously at the desired frequencies in order to find the isolation resistors. At this stage, an optimization process is also needed to solve for the isolation resistors.

The above analysis is quite general. A more detailed analysis for dual-frequency, tri-frequency, and quad-frequency unequal split WPDs are given below. In this way, the design of a certain type of the proposed WPD can be easily accomplished by specifying the power split ratio (k^2), and the desired design frequencies. Most of the mathematical formulas used to find the transmission line parameters or isolation resistors in the next three sections will be given only for one branch of the divider. The other branch parameters can be found using the same formulas with appropriate changes.

3. DUAL-FREQUENCY UNEQUAL SPLIT WPD

For the dual-frequency design, the WPD shown in Figure 1 has two sections ($N = 2$). The two sections of transmission line transformers are used to account for the dual frequency operation. Our goal is to find the branches parameters ($Z_{a1}, l_{a1}, Z_{a2}, l_{a2}, Z_{b1}, l_{b1}, Z_{b2}, l_{b2}$), and isolation resistors (R_1, R_2) using the even-odd mode analysis.

3.1. Even Mode Analysis

Referring to Figure 2, the two branches can be thought of as two dual-frequency TLTs for which closed form design expressions have been derived in [12]. The characteristic impedances and line lengths for the two sections of branch “a” are given by the following equations [12]:

$$l_{a1} = l_{a2} \tag{5}$$

$$l_{a2} = \frac{\pi}{\beta_1 + \beta_2} \tag{6}$$

$$\alpha = (\tan(\beta_1 l_{a1}))^2 \tag{7}$$

$$Z_{a1} = \sqrt{\frac{Z_a}{2\alpha}(R_{L2} - Z_a) + \sqrt{\left[\frac{Z_a}{2\alpha}(R_{L2} - Z_a)\right]^2 + Z_a^3 R_{L2}}} \tag{8}$$

$$Z_{a2} = \frac{Z_a R_{L2}}{Z_{a1}} \tag{9}$$

where β_1 and β_2 are the phase constants at the design frequencies f_1 and f_2 , respectively. As mentioned earlier, the parameters of the second branch (branch “b”) can be found by changing each subscript “a” to “b”, and R_{L2} to R_{L3} in Equations (5)–(9).

3.2. Odd Mode Analysis

Referring to Figure 3 with $N = 2$, the input admittance seen at the output port 2 is given as follows [10]:

$$Y_{ina} = \frac{1}{R'_2} + \frac{Z_{a2}Z_x + jT_2}{Z_{a2}(1 + jZ_{a2}T_2Z_x)} \quad (10a)$$

$$Z_x = \frac{1}{R'_1} - \frac{j}{Z_{a1}T_1} \quad (10b)$$

where $T_i = \tan(\beta l_i)$. Similar equations can be written for Y_{inb} . Equation (10), along with Equation (3), can be split into two equations for the real and imaginary parts. Solving these two equations, the following expressions for R'_1 , R'_2 can be obtained [10]:

$$R'_1 = \sqrt{BF/AE} \quad (11)$$

$$R'_2 = \frac{F}{D - ER'_1} \quad (12)$$

where $A = Z_{a2}[1 + Z_{a2}T_2/Z_{a1}T_1]$, $B = Z_{a2}$, $C = (Z_{a2}/R_{L2})[1 + Z_{a2}T_2/Z_{a1}T_1]$, $D = Z_{a2}^2T_2/R_{L2}$, $F = R_{L2}D$, and $E = T_2 - Z_{a2}/Z_{a1}T_1$. Similarly, R''_1 and R''_2 can be found. Then, the resistors R_1 and R_2 can be found as: $R_1 = R'_1 + R''_1$ and $R_2 = R'_2 + R''_2$. It should be mentioned that to ensure that the values of these resistors are real and positive, a condition on the ratio between the two design frequencies (f_2/f_1) was derived in [17]. The same condition applies here too. This completes the design of the dual-frequency unequal split WPD.

4. TRI-FREQUENCY UNEQUAL SPLIT WPD

The tri-frequency WPD has three sections of TLTs to perfectly match the output ports at the desired three frequencies. Also, three isolation resistors are used to insure good isolation between the output ports.

4.1. Even Mode Analysis

Referring to Figure 2 with $N = 3$, the two branches can be thought of as two triple-frequency TLTs [15]. We note that in the case of unequal split, the analysis is carried out two times, one for each branch since

each branch has its own parameters. The design equations for the first branch are given as follows [15]:

$$Z_{a2} = \sqrt{Z_{a1}Z_{a3}} \quad (13)$$

$$Z_{a2} = \sqrt{R_{L2}Z_a} = Z_a\sqrt{H} \quad (14)$$

$$H = \frac{R_{L2}}{Z_a} \quad (15)$$

$$l_{a1} = l_{a3} \quad (16)$$

$$a = \sqrt{H} \left(\frac{Z_a}{Z_{a1}} - \frac{Z_{a1}}{Z_a} \right) \quad (17)$$

$$b = \frac{Z_a^2}{Z_{a1}^2} H - \frac{Z_{a1}^2}{Z_a^2} \quad (18)$$

$$l_{a2} = \frac{1}{\beta_1} \left[\arctan \left(\frac{(1+H) \cot(\beta_1 l_{a1}) - b \tan(\beta_1 l_{a1})}{2a} \right) \pm p\pi \right] \quad (19)$$

$$u_1 = \frac{\arctan \left(\frac{(1-H) \cot(u_1 \beta_1 l_{a1}) - b \tan(u_1 \beta_1 l_{a1})}{2a} \right) \pm p\pi}{\arctan \left(\frac{(1-H) \cot(\beta_1 l_{a1}) - b \tan(\beta_1 l_{a1})}{2a} \right)} \quad (20)$$

$$u_2 = \frac{\arctan \left(\frac{(1-H) \cot(u_2 \beta_1 l_{a1}) - b \tan(u_2 \beta_1 l_{a1})}{2a} \right) \pm r\pi}{\arctan \left(\frac{(1-H) \cot(\beta_1 l_{a1}) - b \tan(\beta_1 l_{a1})}{2a} \right)} \quad (21)$$

where $u_1 = f_2/f_1$ and $u_2 = f_3/f_1$. The frequencies f_1 , f_2 , and f_3 are the design frequencies. An optimization process is needed to solve Equations (20) and (21) simultaneously. The particle swarm optimization (PSO) technique is used here to obtain the optimum values of Z_{a1} and l_{a1} . The remaining design parameters (the impedances and the lengths) can be obtained using Equations (13)–(19).

4.2. Odd Mode Analysis

Referring to Figure 3 with $N = 3$, the input admittance seen by the output port 2 is given as follows [8].

$$Y_{ina} = G_3 + Y_{a3} \frac{Y_x + jY_{a3} \tan(\theta_3)}{Y_{a3} + j \tan(\theta_3) (Y_x)} \quad (22a)$$

$$Y_x = G_2 + Y_{a2} \frac{G_1 + j(Y_{a2} \tan(\theta_2) - Y_{a1} \cot(\theta_1))}{Y_{a2} + Y_{a1} \cot(\theta_1) \tan(\theta_2) + jG_1 \tan(\theta_2)} \quad (22b)$$

$$\theta_1 = \beta l_{a1}, \quad \theta_2 = \beta l_{a2}, \quad \theta_3 = \beta l_{a3} \quad (23)$$

$$G_1 = \frac{1}{R'_1}, \quad G_2 = \frac{1}{R'_2}, \quad G_3 = \frac{1}{R'_3} \quad (24)$$

$$Y_{a1} = \frac{1}{Z_{a1}}, \quad Y_{a2} = \frac{1}{Z_{a2}}, \quad Y_{a3} = \frac{1}{Z_{a3}} \quad (25)$$

Similar expressions can be obtained for the input admittance looking into the other branch. By imposing the matching conditions (Equations (3) and (4)) simultaneously at the three design frequencies, the isolation resistors can be found using the PSO technique.

5. QUAD-FREQUENCY UNEQUAL SPLIT WPD

The quad-frequency unequal split WPD has two TLTs each composed of four transmission line sections. Moreover, four resistors are used to enhance the isolation between the output ports.

5.1. Even Mode Analysis

Referring to Figure 2 with $N = 4$, the parameters of the four sections TLT in branch “a”, can be found using the following expressions [16]:

$$2a + b \frac{\tan(\beta_1 l_{a4})}{\tan(\beta_1 l_{a3})} + c \frac{\tan(\beta_1 l_{a3})}{\tan(\beta_1 l_{a3})} + d \cdot W + \frac{(H - 1)}{W} = 0 \quad (26a)$$

$$W = \tan(\beta_1 l_{a4}) \cdot \tan(\beta_1 l_{a3}) \quad (26b)$$

$$a = \left(\frac{z_{a3}}{z_{a4}} - \frac{z_{a4}}{z_{a3}} H \right) + \left(\frac{H}{z_{a3} z_{a4}} - z_{a3} z_{a4} \right) \quad (27)$$

$$b = \frac{H}{z_{a4}^2} - z_{a4}^2 \quad (28)$$

$$c = \frac{H}{z_{a3}^2} - z_{a3}^2 \quad (29)$$

$$d = \frac{z_{a4}^2}{z_{a3}^2} H - \frac{z_{a3}^2}{z_{a4}^2} \quad (30)$$

where $H = R_{L2}/Z_a$, $z_{a3} = Z_{a3}/Z_a$, and $z_{a4} = Z_{a4}/Z_a$. Equation (26) should be satisfied at the four design frequencies f_1 , f_2 , f_3 , and f_4 , which results in four non-linear equations that are solved using the PSO technique. The other design parameters can be then calculated using the antimetry conditions [16]:

$$l_{a1} = l_{a4}, \quad l_{a2} = l_{a3} \quad (31)$$

$$Z_{a2} Z_{a3} = Z_{a1} Z_{a4} = Z_a R_{L2} \quad (32)$$

5.2. Odd Mode Analysis

Referring to Figure 3 with $N = 4$, the input admittance seen by output port 2 is given by the following expression [9]:

$$Y_{ina} = G_4 + Y_{a4} \frac{Y_y + jY_4 \tan(\theta_4)}{Y_{a4} + jY_y \tan \theta_4} \quad (33a)$$

$$Y_y = G_3 + Y_{a3} \frac{Y_x + jY_{a3} \tan(\theta_3)}{Y_{a3} + jY_x \tan(\theta_3)} \quad (33b)$$

$$Y_x = G_2 + Y_{a2} \frac{G_1 + j(Y_{a2} \tan(\theta_2) - Y_{a1} \cot(\theta_1))}{Y_{a2} + Y_{a1} \cot(\theta_1) \tan(\theta_2) + jG_1 \tan(\theta_2)} \quad (33c)$$

where

$$\theta_1 = \beta l_{a1}, \quad \theta_2 = \beta l_{a2}, \quad \theta_3 = \beta l_{a3}, \quad \theta_4 = \beta l_{a4} \quad (34)$$

$$G_1 = \frac{1}{R'_1}, \quad G_2 = \frac{1}{R'_2}, \quad G_3 = \frac{1}{R'_3}, \quad G_4 = \frac{1}{R'_4} \quad (35)$$

$$Y_{a1} = \frac{1}{Z_{a1}}, \quad Y_{a2} = \frac{1}{Z_{a2}}, \quad Y_{a3} = \frac{1}{Z_{a3}}, \quad Y_{a4} = \frac{1}{Z_{a4}} \quad (36)$$

By applying the matching conditions (Equations (3) and (4)), the values of the isolation resistors can be found using the PSO technique.

6. NUMERICAL EXAMPLES

According to the above analysis and design procedure, the design of several unequal split WPDs is introduced using the microstrip line technology. The software Ansoft Designer [18] is used for the circuit simulations presented in this section. In the simulations, dispersion effects are taken into account, while the effects of coupling and all other discontinuities are neglected. An FR-4 substrate, with $\epsilon_r = 4.4$ and substrate thickness $h = 60$ mil is assumed in the simulations. The input port impedance is chosen to be 50Ω . The power split ratio between ports 2 and 3 is chosen to be $k^2 = P_3/P_2 = 2$, which gives (referring to Figures 1 and 2): $Z_a = 150 \Omega$, $Z_b = 75 \Omega$, $R_{L2} = 70.71 \Omega$, and $R_{L3} = 35.35 \Omega$.

6.1. Dual-Frequency WPD

The design frequencies are chosen to be $f_1 = 1$ GHz, and $f_2 = 2$ GHz. Using the analysis described in Section 3, the following design parameters are obtained: $Z_{a1} = 116.59 \Omega$, $Z_{a2} = 90.97 \Omega$, $Z_{b1} = 58.29 \Omega$, $Z_{b2} = 45.48 \Omega$, $l_{a1} = l_{a2} = 60^\circ$, $l_{b1} = l_{b2} = 60^\circ$, where $f_1 = 1$ GHz is the reference frequency. Moreover, $R'_1 = 79.21 \Omega$, $R'_2 =$

$141.87\ \Omega$, $R_1'' = 39.63\ \Omega$, and $R_2'' = 70.86\ \Omega$. Thus, the total isolation resistors are: $R_1 = R_1' + R_1'' = 118.84\ \Omega$, and $R_2 = R_2' + R_2'' = 212.73\ \Omega$.

The simulated scattering parameters for this WPD are shown in Figures 4 and 5. It is clear that the designed divider provides excellent input/output ports matching (return losses), which is better than $-40\ \text{dB}$ for S_{11} and S_{33} , and better than $-55\ \text{dB}$ for S_{22} at the two design frequencies. The isolation performance (S_{23}) is better than $-40\ \text{dB}$ at both design frequencies. Figure 5 shows the insertion losses S_{21} and S_{31} . The values of S_{21} are $-4.97\ \text{dB}$ at f_1 , and $-5.15\ \text{dB}$ at f_2 , which are close to the theoretical value of $-4.77\ \text{dB}$. The values of S_{31} are $-1.95\ \text{dB}$ and $-2.13\ \text{dB}$ at f_1 and f_2 , respectively,

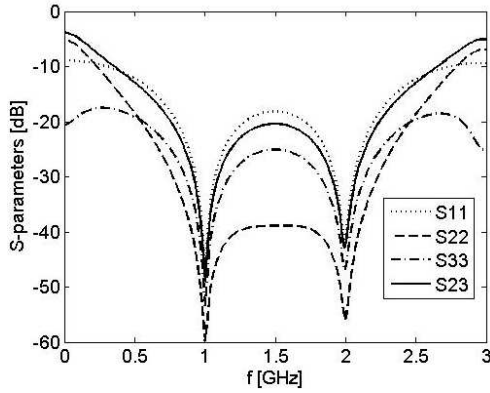


Figure 4. S -parameters for the designed dual-frequency unequal split WPD.

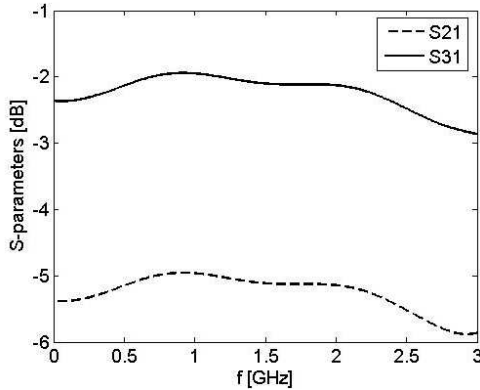


Figure 5. S_{21} and S_{31} parameters for the designed dual-frequency unequal split WPD.

which are also close to the theoretical value of -1.76 dB. The small differences between the simulated and theoretical (ideal) results could be due to the dispersion effects and losses taken into account in the simulations. The designed dual-frequency WPD can be also used as a wide-band divider since it shows good response (return losses and isolation better than -10 dB) in the frequency range 0.5 – 2.5 GHz. It is worth mentioning that the designed dual-frequency WPD shows better isolation performance and output ports matching compared to the structure presented in [3].

6.2. Tri-Frequency WPD

For the tri-frequency WPD, the three design frequencies are chosen as: $f_1 = 1$ GHz, $f_2 = 2$ GHz, and $f_3 = 3$ GHz. From the analysis described in Section 4, the following values for the design parameters are obtained: $Z_{a1} = 124.08 \Omega$, $Z_{a2} = 102.9 \Omega$, $Z_{a3} = 85.49 \Omega$, $Z_{b1} = 62.04 \Omega$, $Z_{b2} = 51.49 \Omega$, $Z_{b3} = 42.73 \Omega$, and $l_{a1} = l_{a2} = l_{a3} = 45^\circ$, $l_{b1} = l_{b2} = l_{b3} = 45^\circ$, where $f_1 = 1$ GHz is the reference frequency. In addition, $R'_1 = 83.54 \Omega$, $R'_2 = 153.27 \Omega$, $R'_3 = 215.07 \Omega$, $R''_1 = 41.79 \Omega$, $R''_2 = 76.52 \Omega$, $R''_3 = 107.59 \Omega$. Thus, the total isolation resistors are: $R_1 = 125.33 \Omega$, $R_2 = 229.79 \Omega$, and $R_3 = 322.86 \Omega$. Figures 6 and 7 show the obtained scattering parameters. The input port return loss S_{11} and output port return loss S_{33} are close to each other and are below -40 dB at the three design frequencies. The output port return loss S_{22} is below -50 dB at these frequencies. Also, the value of the isolation parameter S_{23} is better than -40 dB at the design frequencies. Referring to Figure 7, the insertion loss S_{21} equals -4.99 dB at f_1 ,

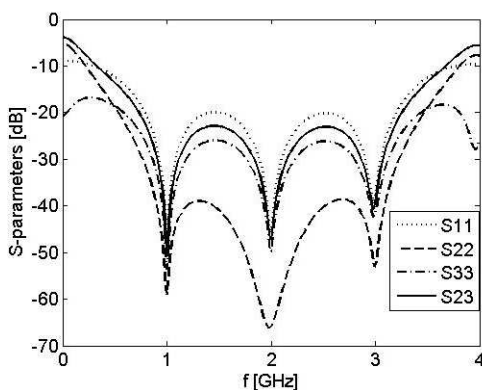


Figure 6. S -parameters for the designed tri-frequency unequal split WPD.

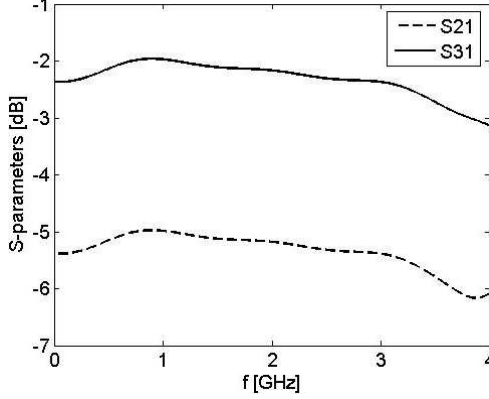


Figure 7. S_{21} and S_{31} parameters for designed tri-frequency unequal split WPD.

-5.18 dB at f_2 , and -5.38 dB at f_3 , while the insertion loss S_{31} equals -1.97 dB at f_1 , -2.17 dB at f_2 , and -2.37 dB at f_3 . These values are close to the theoretical ones: $S_{21} = -4.77$ dB and $S_{31} = -1.76$ dB. As noted in the case of the dual-frequency WPD, the designed tri-frequency WPD can be also used as a wide-band divider working from 0.5 GHz to 3.5 GHz.

6.3. Quad-Frequency WPD

For the quad-frequency WPD, the desired frequencies are $f_1 = 1$ GHz, $f_2 = 2$ GHz, $f_3 = 3$ GHz, and $f_4 = 4$ GHz. From the analysis in Section 5, the following values for the design parameters are obtained: $Z_{a1} = 128.83 \Omega$, $Z_{a2} = 110.94 \Omega$, $Z_{a3} = 95.61 \Omega$, $Z_{a4} = 82.33 \Omega$, $Z_{b1} = 64.42 \Omega$, $Z_{b2} = 55.47 \Omega$, $Z_{b3} = 47.81 \Omega$, $Z_{b4} = 41.18 \Omega$, $l_{a1} = l_{a2} = l_{a3} = l_{a4} = 36^\circ$, $l_{b1} = l_{b2} = l_{b3} = l_{b4} = 36^\circ$, where $f_1 = 1$ GHz is the reference frequency. Moreover, $R'_1 = 86.13 \Omega$, $R'_2 = 160.79 \Omega$, $R'_3 = 225.99 \Omega$, $R'_4 = 290.79 \Omega$, $R''_1 = 43.07 \Omega$, $R''_2 = 80.41 \Omega$, $R''_3 = 113.01 \Omega$, and $R''_4 = 145.42 \Omega$. Thus, the values of the isolation resistors are: $R_1 = 129.2 \Omega$, $R_2 = 241.20 \Omega$, and $R_3 = 339.01 \Omega$, and $R_4 = 436.21 \Omega$. Figures 8 and 9 show the obtained scattering parameters of the designed quad-frequency 1 : 2 WPD. The results can be summarized as follows: at the four design frequencies, the input return loss S_{11} , output return loss S_{33} , and isolation parameter S_{23} are all below -35 dB. The output return loss S_{22} shows a better response with -45 dB at both f_1 and f_4 , and better than -60 dB at the frequencies f_2 and f_3 . The insertion loss S_{21} has the following values: -5 dB at f_1 , -5.21 dB at f_2 , -5.42 dB at f_3 , and

-5.65 dB at f_4 . These values are close to the ideal value of -4.77 dB. On the other hand, the insertion loss S_{31} has the following values: -1.99 dB at f_1 , -2.19 dB at f_2 , -2.41 dB at f_3 , and -2.62 dB at f_4 , which are also close to its ideal value of -1.76 dB. The small differences between the simulated and theoretical (ideal) scattering parameters are due to the same reasons mentioned in the dual-frequency WPD design.

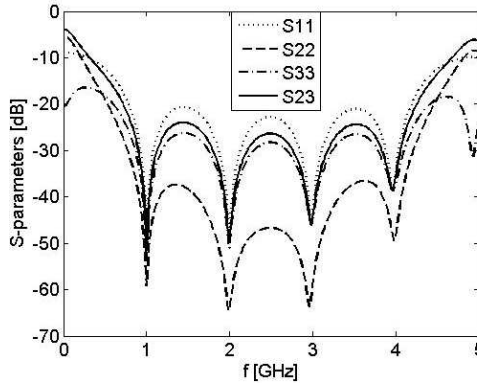


Figure 8. S -parameters for the designed quad-frequency unequal split WPD.

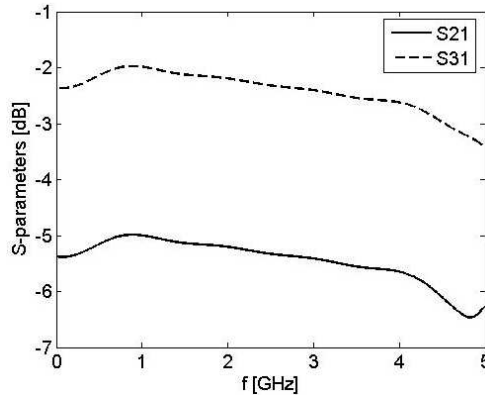


Figure 9. S_{21} and S_{31} parameters for the designed quad-frequency unequal split WPD.

7. EXPERIMENTAL EXAMPLES

In this section, experimental results for several fabricated WPDs are presented. The specifications of the designs are the same as the ones presented in the previous section. The only difference is that they are implemented on a 32 mil thick RO4003C[®] with relative permittivity (ϵ_r) of 3.55 and loss tangent ($\tan \delta$) of 0.0027. The designs are fabricated using a standard milling machine and measured using an Agilent 8510C VNA. Since the VNA has only two ports, a 50Ω load is used to terminate any port that does not contribute to the measurements between the other two ports.

Moreover, the full-wave simulators HFSS [18] and IE3D [19] are used to simulate the designed WPDs. In the full-wave analysis, the coupling effects between the adjacent microstrip traces and discontinuities effects caused by junctions and corners are all taken into account. In HFSS, the analysis is first carried out without the lumped resistors. Then, the resulting scattering parameters are exported to Ansoft Designer [18], where the structure is modified by adding the lumped resistors. Finally, the modified structure is re-simulated to obtain the S-parameters for the designed WPD. In IE3D, the resistors are directly included in the simulation. Each resistor is modeled as a 1 mm side long square made of a thin film resistive material, which has a resistance in $[\Omega/\text{sq}]$. This resistance is defined by the user to achieve the desired value of the resistor. For example, a 100Ω resistor can be modeled as a square made of $100 \Omega/\text{sq}$ resistive material. This model has been verified by simulating a square that represents a series resistor. The simulated S-parameters for the model agree fairly well with the expected S-parameters for a series load [2].

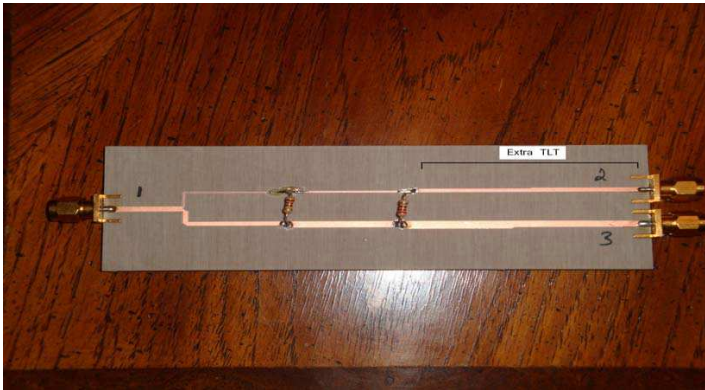


Figure 10. Photograph of the fabricated 1 : 2 dual-frequency WPD.

A photograph of the fabricated dual-frequency WPD is shown in Figure 10. Two extra dual-frequency TLTs are used at the output ports to match the output ports impedances to the $50\ \Omega$ coaxial connectors. These dual-frequency TLTs are designed using expressions similar to Equations (5)–(9). Similar TLTs are used in the fabricated tri-frequency and quad-frequency WPDs. Specifically, two extra triple-frequency three-section TLTs are used in the fabricated tri-frequency WPD, while two extra quad-frequency four-section TLTs are used in the quad-frequency WPD. Referring to Figure 10, the widths and physical lengths of the transmission line sections are given as follows: for the first branch: $W_{a1} = 0.28\ \text{mm}$, $W_{a2} = 0.55\ \text{mm}$, $l_{a1} = 31.85\ \text{mm}$, and $l_{a2} = 31.31\ \text{mm}$. For the second branch: $W_{b1} = 1.38\ \text{mm}$, $W_{b2} = 2.08\ \text{mm}$, $l_{b1} = 30.33\ \text{mm}$, and $l_{b2} = 29.81\ \text{mm}$. For the extra TLT of the first branch: $W_{a1} = 1.2\ \text{mm}$, $W_{a2} = 1.48\ \text{mm}$, $l_{a1} = 30.50\ \text{mm}$, and $l_{a2} = 30.25\ \text{mm}$. For the extra TLT of the second branch: $W_{b1} = 2.56\ \text{mm}$, $W_{b2} = 2.15\ \text{mm}$, $l_{b1} = 29.55\ \text{mm}$, and $l_{b2} = 29.78\ \text{mm}$. To reduce the longitudinal size of these WPDs, curved transmission lines could be used instead of straight ones [9]. Alternatively, one could explore the use of the size reduction techniques presented in [20–22].

Figure 11 shows the measured and full-wave S -parameters for the dual-frequency WPD. The resistance of the lumped resistors used in the fabricated divider was measured and found to be: $R_1 = 117\ \Omega$, and $R_2 = 219\ \Omega$. These are very close to the theoretical values mentioned in Section 6.1; namely: $R_1 = 118.84\ \Omega$, and $R_2 = 212.72\ \Omega$. In the full-wave simulation, the practical values of the resistors are used. The input and output ports return loss parameters (S_{11} , S_{22} and S_{33}), and isolation (S_{23}) are all below $-20\ \text{dB}$ at both $1\ \text{GHz}$ and $2\ \text{GHz}$. A frequency shift of $0.4\ \text{GHz}$ is observed at the second frequency in the measured results of S_{23} . The transmission parameters (S_{21} and S_{31}) are approximately the same as in the circuit model results.

Figure 12 shows the results for the designed tri-frequency WPD. The experimental results are in reasonable agreement with the simulation results. The matching parameters (S_{11} , S_{22} , and S_{33}) are below $-25\ \text{dB}$ at the design frequencies. The isolation between the two output ports shows good performance except at the third design frequency which could be due to the used practical isolation resistor values. The measured transmission parameters (S_{21} and S_{31}) are close to those predicted by the full-wave analysis. The resistance of the lumped resistors used in the fabricated divider was measured and found to be: $R_1 = 118.2\ \Omega$, $R_2 = 235.7\ \Omega$ and $R_3 = 323.1\ \Omega$. These are very close to the theoretical values mentioned in Section 6.2.

Lastly, Figure 13 shows the measured and simulated scattering

parameters for the quad-frequency WPD. It can be seen that good matching and isolation at the desired design frequencies are obtained. Also, good agreement between the simulated and measured

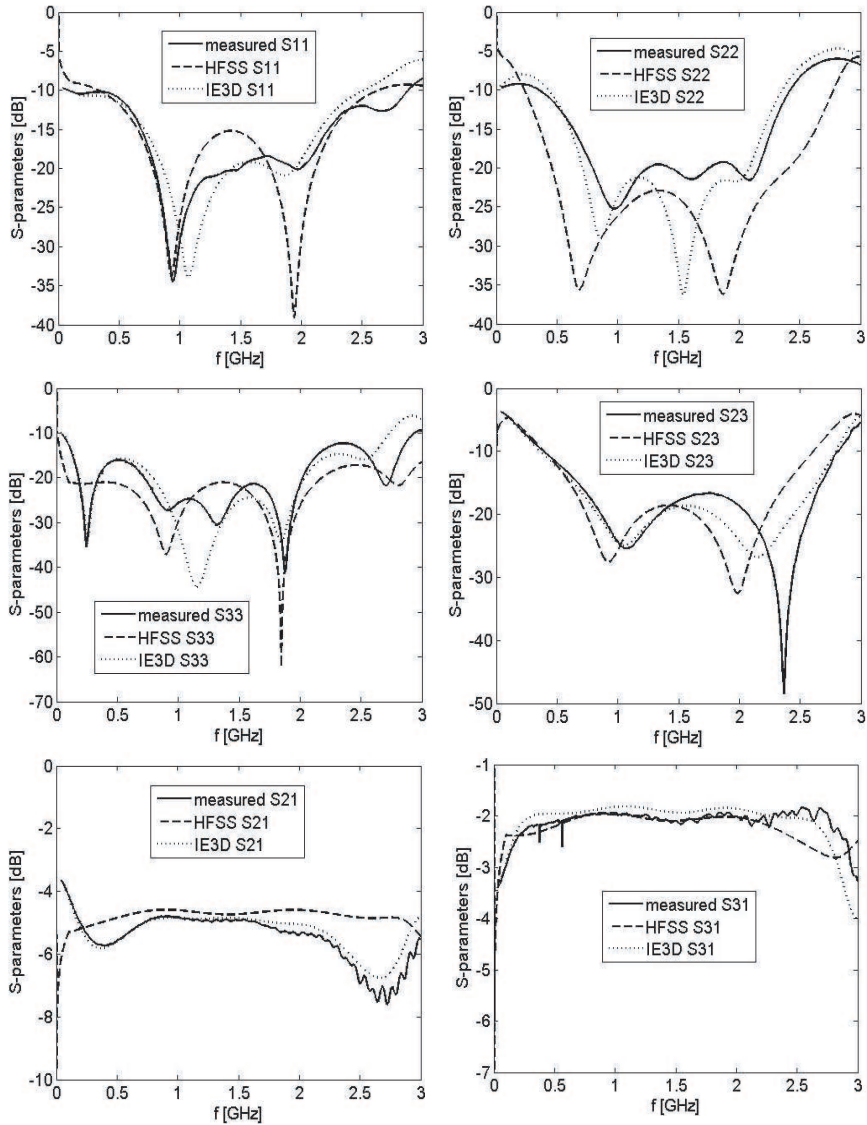


Figure 11. Measured and full-wave analysis results for the fabricated dual-frequency WPD.

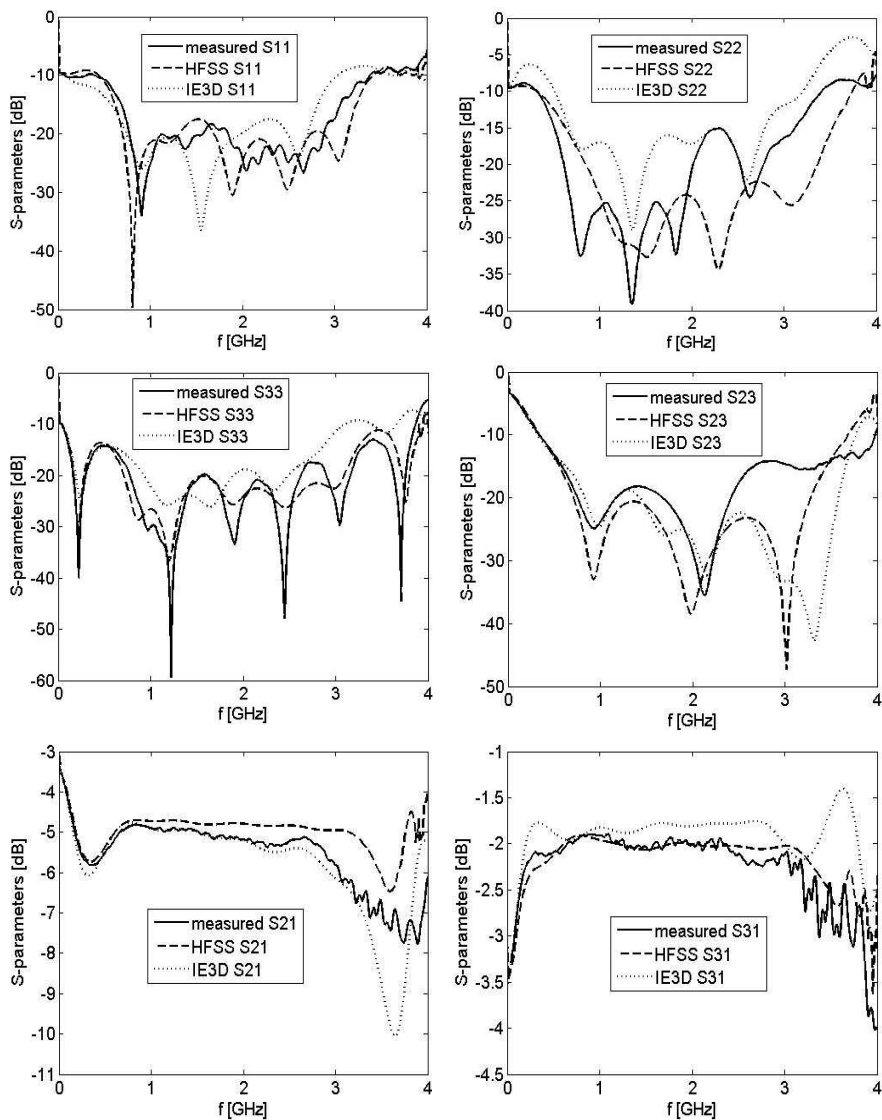


Figure 12. Measured and full-wave analysis results for the fabricated tri-frequency WPD.

transmission parameters (S_{21} and S_{31}) is shown. The resistance of the lumped resistors used in the fabricated divider was measured and found to be: $R_1 = 128.3 \Omega$, $R_2 = 236 \Omega$, $R_3 = 339 \Omega$ and $R_4 = 436 \Omega$. These are very close to the theoretical values mentioned in Section 6.3.

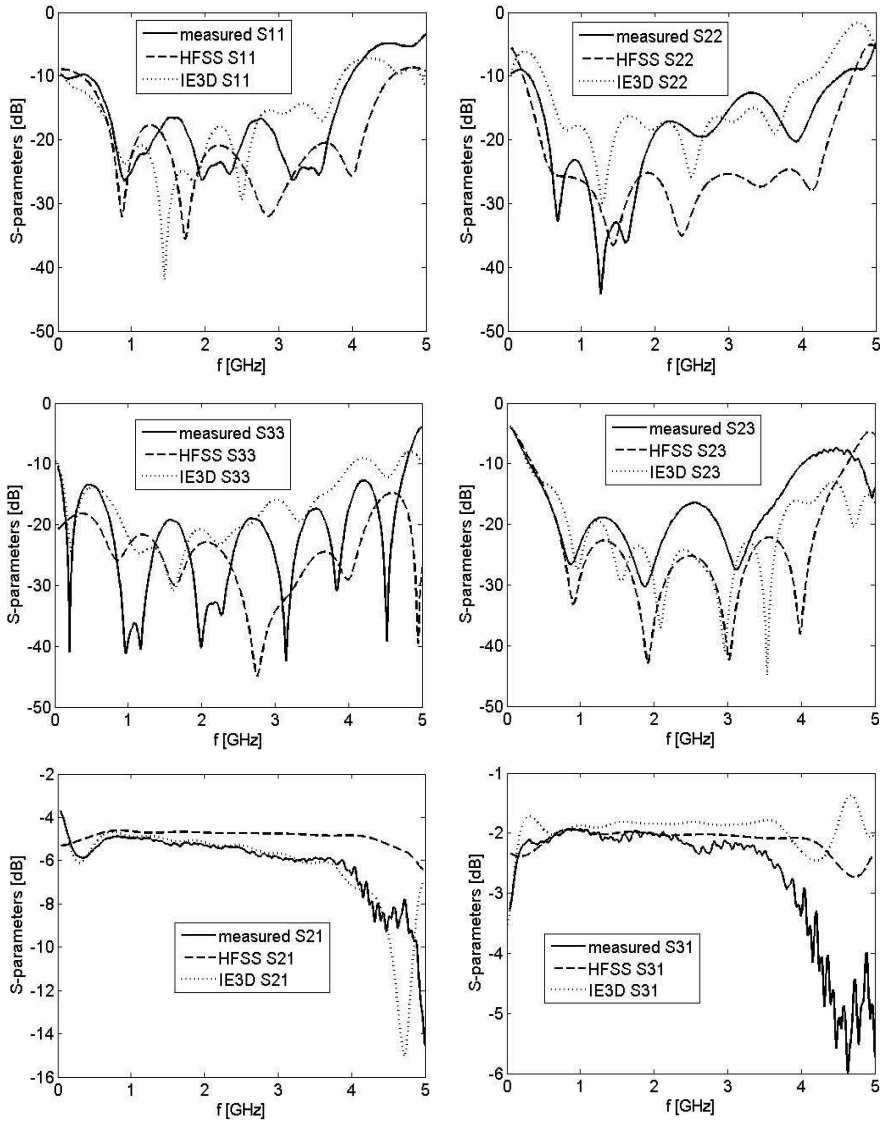


Figure 13. Measured and full-wave analysis results for the fabricated quad-frequency WPD.

In general, the agreement between the experimental results and the simulated ones is acceptable keeping in mind the errors inherent in both the full-wave simulators, and the errors in the experimental results. Modeling the lumped resistors in both simulators does not

exactly reflect their actual physical behavior. Moreover, using carbon resistors (instead of surface mount ones) in the fabricated circuits could have affected the frequency response of the designed WPDs. In spite of this, the fabricated circuits and the obtained experimental results still validate the proposed general design procedure.

8. CONCLUSION

This paper presented the analysis and design of general multi-frequency unequal split WPDs without any significant modification to the original Wilkinson structure (without transmission line stubs or reactive components). The proposed structure and the analytical design method were verified through several power divider examples with different design variables. Specifically, 1 : 2 dual-frequency, triple-frequency, and quad-frequency WPDs were designed, simulated, fabricated and measured. The results of the designed Wilkinson powers dividers showed the validity of the proposed design procedure and proved the multi-frequency (and wide-band) nature of the proposed WPD structure.

REFERENCES

1. Wilkinson, R. J., "An N-way hybrid power divider," *IRE Transactions on Microwave Theory and Techniques*, Vol. 8, No. 1, 116–118, January 1960.
2. Pozar, D. M., *Microwave Engineering*, 3rd edition, John Wiley & Sons, Inc., New York, 2005.
3. Feng, C., G. Zhao, X. liu, and F. Zhang, "A novel dual-frequency unequal Wilkinson power divider," *Microwave and Optical Technology Letters*, Vol. 50, No. 6, 1695–1699, June 2008.
4. Wu, Y., Y. Liu, and S. Li, "A new dual-frequency Wilkinson power divider," *Journal of Electromagnetics Waves and Applications*, Vol. 23, 483–492, 2009.
5. Wu, Y., Y. Liu, and S. Li, "An unequal dual-frequency Wilkinson power divider with optional isolation structure," *Progress In Electromagnetics Research*, Vol. 91, 393–411, 2009.
6. Wu, Y., Y. Liu, and S. Li, "Dual-band modified Wilkinson power divider without transmission line stubs and reactive components," *Progress In Electromagnetics Research*, Vol. 96, 9–20, 2009.
7. Oraizi, H. and A. Sharifi, "Design and optimization of broadband asymmetrical multisection Wilkinson power divider," *IEEE*

- Transactions on Microwave Theory and Techniques*, Vol. 54, No. 5, 2220–2231, May 2006.
8. Chongcheawchamnan, M., S. Patissang, M. Krairiksh, and I. Robertson, “Tri-band Wilkinson power divider using a three-section transmission-line transformer,” *IEEE Microwave and Wireless Communications Letters*, Vol. 16, No. 8, 452–454, August 2006.
 9. Jwaied, H., F. Mawanes, and N. Dib, “Analysis and design of a quad-band Wilkinson power divider,” *Int. Journal on Wireless and Optical Communication*, Vol. 4, No. 3, 305–312, 2007.
 10. Dib, N. and M. Khodier, “Design and optimization of multi-band Wilkinson power divider,” *International Journal of RF and Microwave Computer-Aided Engineering*, Vol. 18, No. 1, 14–20, January 2008.
 11. Robinson, J. and Y. Rahmat-Samii, “Particle swarm optimization in electromagnetics,” *IEEE Transactions on Antennas and Propagation*, Vol. 52, No. 2, 397–407, 2004.
 12. Monzon, C., “A small dual-frequency transformer in two sections,” *IEEE Transactions on Microwave Theory and Techniques*, Vol. 15, No. 4, 1157–1161, April 2003.
 13. Parad, L. and R. Moynihan, “Split-tee power divider,” *IEEE Transactions on Microwave Theory and Techniques*, Vol. 13, 91–95, January 1965.
 14. Khodier, M., N. Dib, and J. Ababneh, “Design of multi-band multi-section transmission line transformer using particle swarm optimization,” *Electrical Engineering Journal (Archiv fur Elektrotechnik)*, Vol. 90, No. 4, 293–300, April 2008.
 15. Chongcheawchamnan, M., S. Patissang, and S. Srisathit, “Analysis and design of a three section transmission line-transformer,” *IEEE Transactions on Microwave Theory and Techniques*, Vol. 53, No. 7, 2458–2462, July 2005.
 16. Jwaied, H., F. Muwanes, and N. Dib, “Analysis and design of quad-band four-section transmission line impedance transformer,” *Applied Computational Electromagnetics Society (ACES) Journal*, Vol. 22, No. 3, 381–387, November 2007.
 17. Wu, Y., Y. Liu, S. Li, C. Yu, and X. Liu, “Closed-form design method of an N-way dual-band Wilkinson hybrid power divider,” *Progress In Electromagnetics Research*, Vol. 101, 97–114, 2010.
 18. Ansoft Corporation, www.ansoft.com.
 19. Zeland Software, www.zeland.com.
 20. Alkanhal, M., “Reduced-size dual band Wilkinson power di-

- viders,” *Proc. Of the Int. Conf. on Computer and Communication Engineering*, 1294–1298, Malaysia, 2008.
21. Lee, Y., I. Park, and C. Shin, “A miniaturized Wilkinson power divider,” *Proc. of APMC*, 37–40, Taiwan, 2001.
 22. Hosseini, F., M. Khalaj-Amir Hosseini, and M. Yazdani, “A miniaturized Wilkinson power divider using nonuniform transmission line,” *Journal of Electromagnetics Waves and Applications*, Vol. 23, 917–924, 2009.